Photoacoustics 31 (2023) 100498

Contents lists available at ScienceDirect

Photoacoustics

journal homepage: www.elsevier.com/locate/pacs

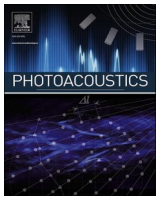

Research article

Elastic and thermo-elastic characterizations of thin resin films using colored picosecond acoustics and spectroscopic ellipsometry

A. Devos [a,*], F. Chevreux [b], C. Licitra [c], A. Chargui [a], L.-L. Chapelon [b]

[a] IEMN – UMR8250 CNRS, Avenue Poincaré BP 69, 59652 Villeneuve d'Ascq, France
[b] STMicroelectronics, Crolles, France
[c] Univ. Grenoble Alpes, CEA, Leti, F-38000 Grenoble, France

ARTICLE INFO

Keywords:
Mechanical properties
Photoresist
Resin
Picosecond acoustics

ABSTRACT

Colored Picosecond Acoustics (CPA) and Spectroscopic Ellipsometry (SE) are combined to measure elastic and thermoelastic properties of polymer thin-film resins deposited on 300 mm wafers. Film thickness and refractive index are measured using SE. Sound velocity and thickness are measured using CPA from the refractive index. Comparing the two thicknesses allows checking consistency between both approaches. The same combination is then applied at various temperatures from 19° to 180°C. As the sample is heated, both thickness and sound velocity change. By monitoring these contributions separately, the Temperature Coefficient on sound Velocity (TCV) and the Coefficient on Thermal Expansion are deduced. The protocol is applied to five industrial samples made of different thin-film resins currently used by microelectronic industry. Young's modulus varies from resin to resin by up to 20%. TCV is large on each resin and varies from one resin to another up to 57%.

1. Introduction

Since the 70 s, polymer resins have been broadly used in the semiconductor industry to achieve patterning by lithography[1]. Resists are materials whose properties change when exposed to ultraviolet (UV) light or electron beams. There are two types of photoresist: positive and negative photoresist. In a positive (resp. negative) tone resist, the region exposed to radiations becomes more (resp. less) soluble allowing it to be removed during the development process. Both kinds of resins are used in the semiconductor industry even if positive photoresists are mostly retained by the semiconductor suppliers due to their higher resolution capabilities.

The conventional photolithographic process uses exposure to UV light (350–430 nm). As diffraction effects limit the minimum size of the device, other lithographic techniques – like electron beam lithography or ion beam lithography – are required to achieve the dimensions for next generation devices. New photoresists are continuously developed to allow reliable structuring in the micron and submicron range. The most commonly used resists are acrylate-based resists such as Poly-Methyl MethAcrylate (PMMA) [2]. Epoxy materials have also many applications in the semiconductor industry; one of its derivatives bis-phenol, a novolac (SU-8), provides high-resolution electron beam patterning [3].

The use of polymers in electronics is not limited to lithography, for example a variety of polymers have been proposed for use as low dielectric constant materials [4]. Polymers are also most widely used as encapsulants and serve as mechanical protection of the circuits, as well as physical barriers against water diffusion.

Thin-film resins are exposed to various processes during the fabrication of devices. It is important to know the elastic and thermo-elastic properties to improve the final reliability of such devices.

For more than 30 years, picosecond acoustics has been opening the field of thin and ultra-thin layers to physical acoustics [5–8]. This ultrafast laser technology implements a pulse-echo technique (like sonar) at the nanoscale. The light absorption of a first femtosecond laser pulse (the pump) leads to the emission of a short acoustic pulse. This pulse propagates in the film at the sound velocity and, at the film/substrate interface, it is partially reflected towards the surface. That returning echo is optically detected using another laser pulse (the probe) time-delayed with respect to the pump pulse. By detecting successive acoustic echoes, we can measure the time-of-flight and deduce the longitudinal sound velocity of the thin-film material from the thickness.

On transparent thin-film materials, both thickness and velocity are measured from refractive index [9]. Indeed, by an appropriate choice of

* Corresponding author.
E-mail address: Arnaud.Devos@iemn.fr (A. Devos).

https://doi.org/10.1016/j.pacs.2023.100498
Received 6 December 2022; Received in revised form 3 April 2023; Accepted 19 April 2023
Available online 20 April 2023

the probe laser wavelength, we can favor another detection regime in which the acoustic propagation itself is monitored as an oscillation. This so-called Brillouin oscillation (BO) is the acousto-optic signature of the transparent material. The BO period is determined by the probe laser-wavelength and the product between refractive index and sound velocity of the material through which the acoustic pulse travels [10]. Sound velocity can then be extracted from the measured period and refractive index with no assumption on the film thickness. This is especially interesting for films whose thicknesses are not so well known or made of material in which sound attenuation is especially strong so that no echo returns to the surface after a round trip. This is also interesting for measurement at various temperatures as both thickness and sound velocity vary.

Both approaches were previously applied to thin polymer films. A very early study by Morath et al. measured the elastic properties and damping in PMMA using a pulse-echo scheme [11]. In the case of an ultra-thin layer, the femtosecond laser excites the resonance of the whole layer, and the pulse-echo signal is replaced by complex oscillations. This was recently used to investigate elastic properties [12] and the glass transition of ultra-thin PMMA films [13]. BO has also been used to investigate elastic properties of polymers [14,15].

Laser-wavelength plays an important role in the optical detection of picosecond acoustic pulses [16]. Some contributions can be reinforced by carefully choosing the probe wavelength range. For example, BO in silicon is much easier to detect in the blue range than in the near infrared [17]. The dependence of the frequency or amplitude of some acousto-optic contributions with laser wavelength can also be used to confirm the exact nature of such a contribution. For example, the BO period varies linearly with the probe wavelength if one neglects the influence of dispersion. We designate as 'Colored Picosecond Acoustics' (CPA) the combination of a picosecond acoustic setup with a tunable laser source. The laser is tuned to take advantage of these wavelength effects to support an interpretation, to extract more parameters, to achieve higher accuracy or to be compatible with more materials[16].

In this paper, we present a protocol that combines CPA and Spectroscopic Ellipsometry (SE) to measure sound velocity and thickness of any polymer thin-film resin at various temperatures. A SE measurement provides refractive index and thickness. From the refractive index, CPA is used to extract sound velocity and thickness. The consistency of our approach is confirmed by a comparison between the two thicknesses. The efficiency of the protocol is demonstrated by applying it to five industrial samples made of five different polymer thin-film resins currently used in microelectronics at the production level.

In a previous work published by one of the authors, it was proposed to use picosecond acoustic measurements over several angles to simultaneously extract refractive index, film thickness and sound velocity [18]. Such an approach was not applied in the present work for two reasons. First, we wanted to elaborate a metrological protocol compatible with large size wafers with which our variable angle sample holder was not compatible. On the contrary, the spectroscopic ellipsometer we used is designed to work with 300 mm wafers. Second, the accuracy on the refractive index one can reach using the several angles scheme is well below what is obtained using an ellipsometer.

2. Material and methods

2.1. Samples description

To demonstrate the efficiency of the proposed methodology, we applied our measurement protocol to five different photoresists currently used in the microelectronic industry. They differ by their chemical nature, their tone (positive or negative) and their final application. What they all have in common is that they are deposited by spin coating according to a well-established process on a dedicated production tool onto 300 mm silicon wafers. After deposition, the resin is cured to induce polymerization, time and temperature being the key parameters of the process. The thicknesses of the resin films studied in this work depends on the final application and varies from 680 to 2700 nm. Labels and nominal thicknesses of the studied samples are given in Table 1. The resists are divided into three groups designated by the letters A, B and C. The A series is made of the same epoxy acrylate resin based on the industrial-grade bisphenol A-based epoxy resin and acrylic acid, that has been synthesized in order to develop hybrid resin. In group A, resins A1 to A3 differ in curing temperature below 200 °C, at 200 °C and above 200 °C, respectively. Sample B is a pure acrylic negative resin. Sample C is a positive resist based on poly(4-hydroxystyrene) polymer that can be used in extreme UV lithography.

For ellipsometry measurements, the same resins are deposited directly onto 300 mm silicon wafers. For CPA measurements, a 25 nm thick TiN layer is first deposited by chemical vapor deposition onto the 300 mm silicon wafers before spin coating of the resin film.

2.2. Picosecond acoustic setup

In this work, the picosecond acoustic measurements are performed using a two-color pump-probe setup with a commercial femtosecond laser operating in the wavelength range 690–1040 nm [19].

The principle of such a measurement is illustrated in Fig. 1 (inset). The laser output is split into two parts, the pump and the probe. The pump beam is focused on the sample surface and is absorbed in the TiN layer as the resin is transparent to the pump wavelength. The resulting local heating leads to two strain pulses, one propagating in the Si wafer, the other in the resin layer.

The second part of the laser, the probe beam, is first frequency doubled using a β-BaB_2O_4 nonlinear crystal. The resulting blue beam is then focused on the sample surface at the same place but time-delayed with respect to the pump via a mechanical delay-line. The probe light reflected by the sample is monitored by a photodiode. To improve the signal-to-noise ratio, the pump beam is chopped using an acousto-optic modulator and the output of the photodiode is amplified through a lock-in scheme.

Several acousto-optic contributions are detected by the probe and discussed later. One of them is the BO while acoustics and light coexist in the transparent resin layer. When such a pulse reaches the free surface, it is reflected, the strain changes its sign and a sudden change in the optical reflectivity is detected [20].

The zone measured using CPA is defined by the overlap area of the two focused laser beams. The pump and probe beams are focused using a lens with a focal length of 60 mm. At 920 nm, we measure a spot size (full width at half maximum intensity) of 12.5 and 7.5 μm for pump and probe, respectively. To avoid damaging the investigated material, the incident laser average power is reduced to 20 mW and 1.5 mW for pump and probe, respectively. The absorption of the pump produces a maximum transient temperature rise of 15 °C and a steady state temperature change of 0.8 °C[21]. These estimates suggests that the layer is not damaged by the cumulative heating induced by the laser. The measurement is performed in less than one minute and no change in the sample response is observed during signal acquisition. To compare SE and CPA results, both techniques are applied to the wafer center. Furthermore, the CPA signal is obtained by averaging the measurements of 16 points uniformly distributed over a 1 mm^2 zone to better compare with the larger ellipsometry spot size (typically a few mm^2).

The sample is held on a hot plate so that the CPA measurement can be performed at various temperatures from ambient to 180 °C. Temperatures were measured using two sensors. A first one is included in the hot plate and lets us control the temperature of the heating device. But the most important point to know is the sample temperature, which may differ from the heating element temperature due to thermal contact and heat diffusion into the sample itself. To overcome this, thermal paste is used to improve the thermal contact between the back side of the wafer and the hot plate. Another self-adhesive thermocouple is directly sticked on the wafer surface to measure the sample temperature. A shift of less

Table 1
Samples description and results measured by Spectroscopic Ellipsometry (SE) and Picosecond Acoustics (CPA). TCn means Temperature Coefficient on Refractive index, TCV means Temperature Coefficient on Sound Velocity, CTE is the Coefficient of Thermal Expansion. All temperature coefficients are extracted between 19 and 120 °C.

Samples		*Spectroscopic Ellipsometry*				*Colored Picosecond Acoustics*			
Label	Nominal Thickness nm	Refractive index @ 460 nm	Thickness nm	TCn 10^{-6}/°C	CTE 10^{-6}/°C	Sound velocity m/s	Thickness nm	TCV 10^{-6}/°C	CTE 10^{-6}/°C
A1	1100	1.5768	1026	-59	153	2858	1040	-905	122
A2	2000	1.6112	1924	-57	139	2709	1994	-1190	162
A3	2700	1.5778	2640	-68	179	2944	2693	-1419	111
B	680	1.5163	708	-70	105	2810	675	-1379	91
C	1050	1.6156	1134	-40	97	2971	1166	-1028	123

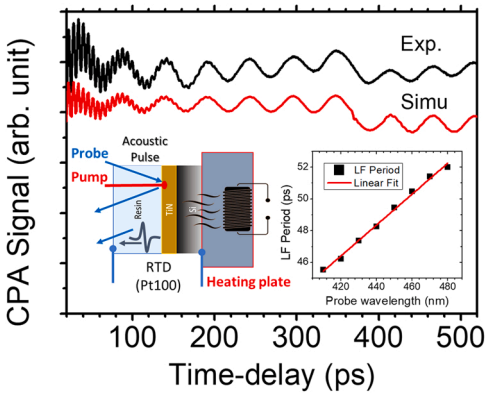

Fig. 1. CPA signal measured on sample A1 compared to a simulation result. A thin resin film is deposited on an ultra-thin TiN layer from where a short acoustic pulse is emitted by the absorption of a laser pulse (pump). Acoustic propagation is monitored using a second optical pulse (probe). Inset: left, scheme of the setup; right, period of the low frequency (LF) oscillation as a function of the probe wavelength.

than 5 °C is found between the two sensors. In the following, we use the temperature measured at the sample surface to plot the results. During the heating, 10 min were given between two temperature steps to let the system thermalize.

2.3. Spectroscopic ellipsometry

Spectroscopic ellipsometry (SE) measurements were performed over a wide spectral range (210–2500 nm) using a dual rotating compensator ellipsometer (Woollam RC2 instrument). Temperature-dependent ellipsometry measurements were performed on small samples in a Linkam heat cell purged with nitrogen. The ellipsometer beam intensity was lowered using neutral filters and shuttered between measurements to ensure that the polymer was not damaged by light and that the measurements were reproducible. Heating and cooling rates were 1 °C/min.

Depending on the material, the film thickness and optical constants were extracted using a Cauchy model applied in the transparent region or a sum of Tauc-Lorentz and Gaussian oscillators. Temperature-dependent measurements were analyzed using the forementioned dispersion laws on top of the silicon substrate with temperature dependent optical constants.

Measurements were performed at the wafer center, the spot size being 3 mm × 8 mm.

3. Results and discussion

3.1. Typical CPA signal at RT

Fig. 1 presents a typical acoustic signal measured on the sample A1 (wafer center) using the femtosecond laser centered at 920 nm. The thermal background due to the heating of the sample by the pump beam has been removed for clarity. TiN is expected to absorb the pump light since the photoresist layer is transparent. This would launch an acoustic pulse simultaneously into the Si substrate and the resin whose signatures would immediately begin at zero delay given the small thickness of the TiN and its fast sound velocity (10770 m/s) [22]. The magnitude of the strain pulse emitted by the TiN layer is estimated to be 1.2×10^{-4} from the maximum temperature rise induced by the pump absorption[23].

A high frequency (HF) oscillation is observed within the first 100 ps while a low frequency (LF) signal is present over the entire range. Both oscillations are BO related to an acousto-optic interaction within the sample as probe light reflects off the travelling acoustic pulses and interferes with the probe light reflected from interfaces within the stack. At normal incidence, the oscillation period T_{BO} of the BO is related to the refractive index n and sound velocity ν of a material as well as the probe wavelength λ_{probe} according to:

$$T_{BO} = \frac{\lambda_{probe}}{2n\nu}. \quad (1)$$

At $\lambda_{probe} = 460$ nm, Si exhibits $n = 4.58$; given $\nu_{Si} = 8430$ m/s, Eq. 1 gives $T = 5.94$ ps which corresponds very well with the measured value of 5.93 ps for the HF part[24,25]. The exponential decay of the HF signal is in-line with previous reports of the strong acoustic damping observed in Si for blue/UV wavelengths due to direct interband transitions in this range [17]. The LF signal is also expected to correspond to BO but detected in resin. Since the resin presents a lower refractive index and a much lower elastic modulus, the period should be significantly higher. A period of about 50 ps is measured, with $n = 1.6$ we get $\nu_{Resin} = 2900$ m/s. The transparency of the resin is consistent with the constant amplitude of the LF signal during hundreds of picoseconds.

A sudden change in the amplitude of the measured signal is detected around 360 ps. This time-delay corresponds to the arrival of the strain pulse at the free surface where it is reflected and sign changed. From compressive to extensive, the strain pulse then propagates back towards the substrate. The sign change of the strain pulse induces a reflectivity step, whose amplitude is sensitive to the laser wavelength[15,26]. This contribution allows us to measure the acoustic time-of-flight in the resin layer and to deduce its thickness from measured velocity. Thanks to the previous estimation of the sound velocity from BO, we obtain a thickness of 1044 nm from the 360 ps time-of-flight, which corresponds to the expected thickness of the resin film.

To support the previous interpretation, we performed similar measurements but at different laser-wavelengths. First, when the laser is tuned from 780 to 960 nm, the HF and LF oscillations change in frequency according to Eq. (1) confirming their BO nature. The change in LF period as a function of probe wavelength can be seen in the inset of Fig. 1. Such a dependence is especially important in confirming the BO nature of the LF oscillation because in a previous report on similar materials, oscillations detected in the transient reflectivity were related to a thickness resonance of the resin layer[12]. If a similar contribution had been detected in the present case, no influence of the laser wavelength on the measured period would have been observed. Secondly, the

amplitude of the 360 ps sudden change varies as the laser is tuned and even undergoes a sign change, as expected for a reflectivity step[26]. While at 920 nm the signal at 360 ps presents a downward step (Fig. 1), at 880 nm the same step is upward.

For a further understanding of the origin of these signals, numerical simulations were performed according to the theories of acoustic generation, propagation and detection as previously elaborated by others [27]. When known, the values of n, ν, and mass density ρ were used for each layer without change from literature [24,25,28], while those that were not known were deduced through the simulation by considering the quality of the overlap of the simulated signal to the measured one. The excellent fit shown in Fig. 1 between simulation and experiment is then used to accurately extract the sound velocity and thickness of the resin layer from the refractive index measured by ellipsometry.

3.2. Various resins, different elasticities

Following the same protocol for each sample, we extracted sound velocity and thickness from the refractive index. A few CPA traces are reproduced in Fig. 2, all of which show the same contributions as discussed above: HF oscillation, LF oscillation and a reflectivity step. From one sample to another, the reflectivity step is detected at different time-delays because the resin thickness differs from sample to sample.

The thickness measured by ellipsometry at the center of the wafer can then be compared to the CPA thickness. Fig. 2 presents a correlation between these values. An excellent correlation is obtained between the two approaches, which finally validates the whole extraction.

Regarding the sound velocity, there are some differences between the samples. A 9% difference is found between the sound velocities which corresponds to a 20% difference to the Young's modulus. Different elasticities are expected for different polymers, but it is found that the deposition and curing parameters also play an important role in the final elastic properties of the resin (differences between samples of series A). This illustrates the major interest of being able to characterize any resist as deposited under real conditions.

3.3. Temperature effects on resins

In Fig. 3, we compare the CPA response of the same A1 sample measured at room temperature and at 100 °C. Heating the sample has two distinct effects. First, one notes a change in the reflectivity step delay: at 100 °C, the step changes to a longer delay of about 30 ps. This means that the acoustic time-of-flight increases as the sample is heated. This is the result of two effects, thermal expansion and reduction of sound velocity.

Second, the acousto-optic signature is also affected by sample heating. In Fig. 3, we draw a box containing 2.5 complete cycles of the BO on each trace. This reveals that the oscillation period is smaller at high temperature than at room temperature (box size is 3.8 ps larger at 100 °C than at 19 °C). This means that temperature induces a decrease

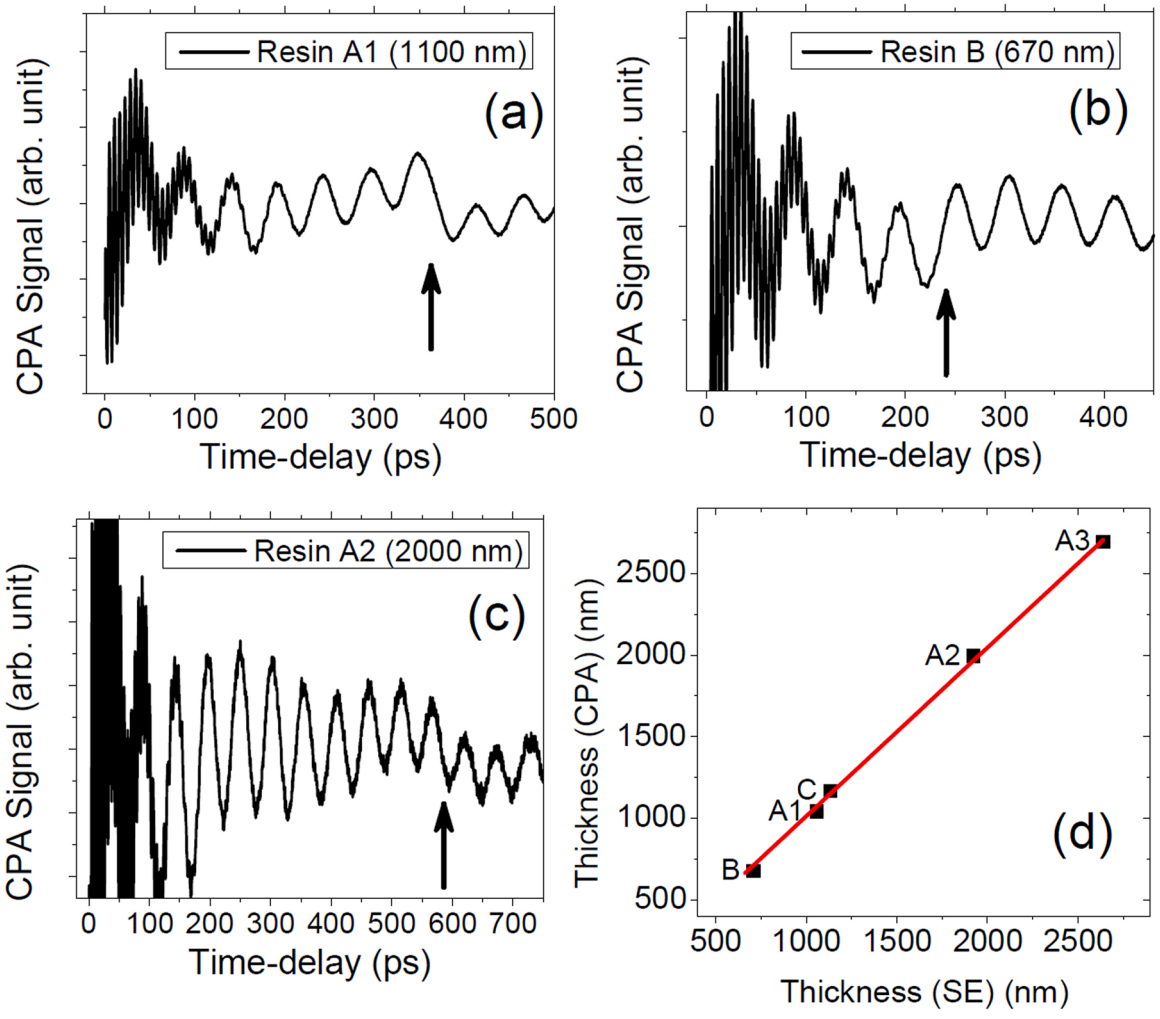

Fig. 2. (a) to (c) CPA signal obtained on three resin samples with different thicknesses (sample A1, B & A2 respectively). (d) Correlation between thickness measured using Colored Picosecond Acoustics (CPA) and Spectroscopic Ellipsometry (SE).

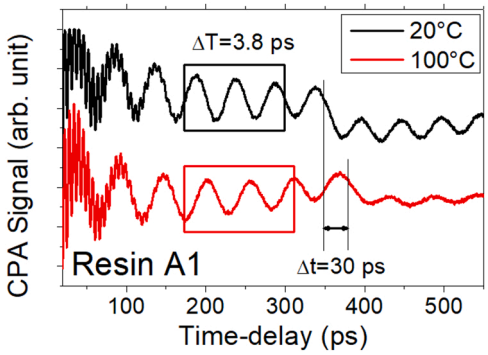

Fig. 3. Comparison between the CPA signal measured on sample A1 at room temperature and at 100 °C. The reflectivity step detected at the arrival of the acoustic pulse at the free surface is shifted to a longer delay. Brillouin oscillation detected during propagation in the resin film is also affected by the sample heating. This is highlighted by the comparison of the boxes that contain 2.5 periods of the Brillouin signal.

of the *nv* product.

We took advantage of the strong sensitivity of the BO period to temperature to verify that there is no cumulative heating induced by the laser. To do so, we compared the signal measured using half the pump power to the original signal (full pump power). According to the result shown in Fig. 3, a change of 10 °C in the resin would lead approximately to a 0.5 ps change in the oscillation period. This means a time-shift of 3 ps after six complete cycles, a value that would have been easy to detect. However, the only differences observed were to the signal amplitude and the signal to noise ratio, both degraded by the decrease of the pump power as expected. The amplitude is reduced by a factor of two as is the pump power, which first confirms that the measurement is performed in the linear regime. This also demonstrates that the measurement is non-destructive.

Neglecting first any change in the refractive index, the reduction in the sound velocity can be deduced from the change in the oscillation period. The shift of the delay at which the acoustic pulse reaches the free surface at 100 °C, is then estimated to 27 ps. Thus, among the 30 ps of total measured shift of the time-delay, only 3 ps are related to thermal expansion of the resin layer. Roughly, only ten percent of the effect on time-of-flight is thus due to thermal expansion.

The previous extraction was based on an assumption of an unchanged refractive index. In reality, temperature has also an effect on the optical properties of the resin layer. SE at variable temperature was used to monitor the variation of refractive index and thickness with temperature between 20 °C and 180 °C. The refractive index measured on the sample A1 at various temperatures is plotted in Fig. 4. As expected, a small decrease of the refractive index is found as the sample is heated. The data fit reasonably well with a linear model, allowing us to

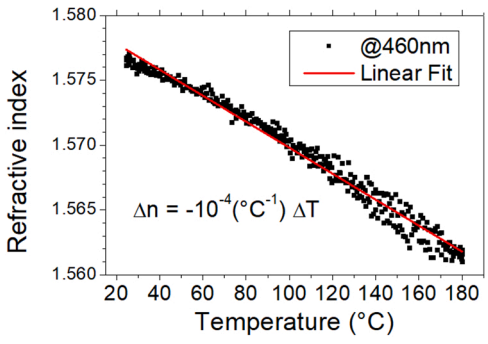

Fig. 4. Refractive index measured by spectroscopic ellipsometry at various temperatures. Experimental data are fitted using a linear fit from which the Temperature Coefficient on Index (TCn) is deduced.

quantify the index change as follows: $\Delta n = -10^{-4}\,(^{\circ}C^{-1})\Delta T$ where ΔT is the temperature change of the sample. In the case of data shown in Fig. 4, one expects a change from 1.577 to 1.569 (0.5%) in refractive index between 20 and 100 °C in resin A1. Such a result confirms that temperature has a stronger effect on the sound velocity than on the refractive index.

3.4. All quantitative results

We now extract some thermo-elastic parameters of the 5 resins by combining the SE and CPA results at different temperatures. To achieve this, we first compute the relative variation of sound velocity d*v*/*v* and relative variation of thickness (d*e*/*e*) from the relative change in refractive index (d*n*/*n*), Brillouin period (dT_{BO}/T_{BO}) and the relative change in acoustic time-of-flight (dτ/τ). For that, we differentiate the fundamental equations, Eq. (1) and e=*v*τ:

$$dv/v = -(dn/n) - (dT_{BO}/T_{BO}) \quad (2)$$

$$de/e = dv/v + d\tau/\tau. \quad (3)$$

d*v*/*v* is negative in the present case as for any material except silica [29], the sound velocity decreases as the temperature increases. In Eq. (3), d*e*/*e* is the sum of two contributions of opposite signs. As the temperature increases, the arrival at free surface is time-delayed but as a combination of two effects, the sound velocity decreases and the thickness thermal expands.

We then calculate *T Cn* , *TCV* and *CTE* which are the coefficients of variation with temperature of refractive index, sound velocity and film thickness, respectively. Such quantities are ideal for comparing different materials.

$$TCn = (dn/n)/\Delta T \quad (4)$$

$$TCV = (dv/v)/\Delta T \quad (5)$$

$$CTE = (de/e)/\Delta T \quad (6)$$

All quantities are given in $^{\circ}C^{-1}$ unit.

Two *CTE* values can be extracted from our measurements: one from SE which extracts the resin thickness at various temperatures; the other from CPA assuming the refractive index measured by SE. All the results are compiled in Table 1.

3.5. Discussion

The first point to be noted about the results in Table 1 is the high value obtained for the *TCV* on each sample. In the range of − 800 to − 1200 × 10^{-6}/°C, *TCV* is more than eight times greater than *CTE*. This confirms that the shift of the acoustic time of flight induced by temperature is mainly governed by a change in velocity compared to the thermal expansion effect. The *TCV* of resins is also found to be large compared to other materials: silica for example exhibits a *TCV* of + 70 to + 100 × 10^{-6}/°C (*TCV* is positive in silica, sound velocity increases at higher temperature) [29]; aluminum, which is known to be a high *TCV* metal, reaches − 250 to − 300 × 10^{-6}/°C more than three times lower than any resin measured here [30].

In spite of this, our values are within the expected range for such materials. In the literature, one finds an estimate of d*v*/d*T* value for PMMA in the range of − 3.2 m/s°C [31]. Divided by a typical sound velocity *v*, we obtain a TCV value close to − 1100 × 10^{-6}/°C.

From one resin to another, we note significant variations in the TCV parameter, which seems to be more material dependent than was found for the sound velocity. Sample A3 presents a TCV 57% higher than sample A1. Such variations justify the need for an accurate measurement of elastic and thermoelastic parameters.

Finally, CTE is found in the range of + 0.9 to + 1.6 × 10^{-4}/°C which is somewhat lower than previously reported values, generally above

$2 \times 10^{-4}/°C$.

4. Conclusion

We present a protocol to measure the longitudinal sound velocity and its temperature dependence of polymer resin thin films. To this end, we combined an ultrafast time-resolved technique and ellipsometry performed at different temperatures. We applied such a protocol to a series of five samples made from five different resins currently used in microelectronics.

SE measures the refractive index and film thickness. CPA deduces the sound velocity and thickness from the SE refractive index. The good agreement between the two thickness values attests to the consistency of the extraction scheme. Sound velocity is found to vary from one sample to another in the range of 10% which means a variation of Young's modulus of typically 20%. As the sample is heated, refractive index, thickness and sound velocity are affected and we use the presented protocol to quantify the temperature change in each parameter. Elasticity is found to be the most sensitive parameter to heating, which is quantified through the Temperature Coefficient on Velocity (TCV). All resins present a large TCV value, in the range between -900 and $-1400 \times 10^{-6}/°C$. The contrast ratio from sample to sample is stronger on TCV than on elasticity with a variation up to 57% on TCV. The coefficient of thermal expansion (CTE) is also extracted from both experimental approaches. Future work will take advantage of such a protocol to track the phase transition that polymer materials are expected to present above a critical value. Above such a transition temperature, TCV and CTE are expected to drastically change which could be identified thanks to the quantitative and non-destructive extraction we have developed.

Declaration of Competing Interest

The authors declare that they have no known competing financial interests or personal relationships that could have appeared to influence the work reported in this paper.

Data Availability

Data will be made available on request.

Acknowledgements

The authors acknowledge funding support within the frame of the STMicroelectronics-IEMN common laboratory and the NANO2022 Program. Part of this work, performed on the Platform for Nano-Characterisation (PFNC) of CEA, was supported by the "Recherche Technologique de Base" Program of the French Ministry of Research.

References

[1] A. Soyano, Int. Polym. Sci. Technol. 39 (2012) 33.
[2] F. Rahman, D.J. Carbaugh, J.T. Wright, P. Rajan, S.G. Pandya, S. Kaya, Microelectron. Eng. 224 (2020), 111238.
[3] E. Sharma, R. Rathi, J. Misharwal, B. Sinhmar, S. Kumari, J. Dalal, A. Kumar, Nanomaterials 12 (2022) 2754.
[4] G. Maier, Mater. Today 4 (2001) 22–33.
[5] H.T. Grahn, H.J. Maris, J. Tauc, IEEE J. Quantum Phys. 25 (1989) 2562.
[6] G.A. Antonelli, B. Perrin, B.C. Daly, et al., MRS Bull. 31 (2006) 607–613.
[7] O. Matsuda, M.C. Larciprete, R. Li Voti, O.B. Wright, Ultrasonics 56 (2015) 3.
[8] V.E. Gusev, P. Ruello, Appl. Phys. Rev. 5 (2018), 031101.
[9] A. Devos, R. Cote, G. Caruyer, A. Lefebvre, Appl. Phys. Lett. 86 (2005), 211903.
[10] C. Thomsen, H.T. Grahn, H.J. Maris, J. Tauc, Opt. Comm. 60 (1986) 55.
[11] C.J. Morath, H.J. Maris, Phys. Rev. B 54 (1996) 203.
[12] D. Brick, M. Hofstetter, P. Stritt, J. Rinder, V. Gusev, T. Dekorsy, M. Hettich, Ultrasonics 119 (2022), 106630.
[13] A.V. Akimov, E.S.K. Young, J.S. Sharp, V. Gusev, A.J. Kent, Appl. Phys. Lett. 99 (2011), 021912.
[14] P. Poncet, F. Casset, A. Latour, F.D. dos Santos, S. Pawlak, R. Gwoziecki, A. Devos, P. Emery, S. Fanget, Actuators 6 (2017) 2–11.
[15] J. Costa Dantas Faria, P. Garnier, A. Devos, Appl. Phys. Lett. 111 (2017), 243105.
[16] A. Devos, Ultrasonics 56 (2015) 90.
[17] A. Devos, R. Côte, Phys. Rev. B 70 (2004), 125208.
[18] R. Côte, A. Devos, Rev. Sci. Instrum. 76 (2005), 053906.
[19] Chameleon Ultra II from Coherent Inc, Santa Clara, CA 95054.
[20] O.B. Wright, Opt. Lett. 16 (1991) 1529.
[21] Following S. Kashiwada et al. in J. of Appl. Phys. 100, 073506 (2006),the maximum temperature rise can be estimated using the expression Q(1-R)/(ArCz), where Q is the pulse energy (0.25 nJ), R is the opticalreflectance at the pump wavelength (typically 0.7), A is the pump beamspot area, r is the mass density (5210 kg/m3), Cis the specific heat capacity per unit mass [600 J/(kg °C) from W. Lengauer, S.Binder, K. Aigner, P. Ettmayer, A. Guillou, J. de Buigne, G. Groboth, Journalof Alloys and Compounds. 217: 137–147 (1995)] and z the optical penetration length in TiN (18 nm assuming an imaginary partof the optical index at 920 nm in TiN close to 4 [28]; 25 nm if one considersthat due to electron diffusion in TiN all the layer is excited by the pump). Combining all these values leads to a maximumtemperature rise of ~11-15°C. The steady-state temperature rise is governed bythe pump power (20 mW 50% chopped) and the thermal conductivity of the silicon substrate[148 W/(m °C)]. At the center of the pump beam, it is estimated to be 0.8°C.
[22] T. Lee, K. Ohmori, C.S. Shin, D.G. Cahill, I. Petrov, J.E. Greene, Phys. Rev. B 71 (2005), 144106.
[23] The magnitude of the strain pulse A is estimated from thermal expansion induced by the maximum temperature rise ΔT itself due to the absorption of the pump (15°C see [21]) using the formula: $A=\Delta T * 3B\beta/(\rho v^2)$, where B is the bulk modulus [251 GPa, from D.S. Stone et al. in Journal of Vacuum Science & Technology A 9, 2543 (1991)], β the thermal expansion coefficient [$9.4\times10^{-6}/°C$ from Andrew William in Handbook of Refractory Carbides and Nitrides: Properties, characteristics, processing, and applications, edited by Hugh O. Pierson (1996)], ρ is the mass density (5210 kg/m^3) and v the longitudinal sound velocity (10770 m/s [22]).
[24] D.E. Aspnes, A.A. Studna, Phys. Rev. B 27 (1983) 985.
[25] B.A. Auld, Acoustic fields and waves in solids R.E. Krieger (1990).
[26] A. Devos, J.-F. Robillard, R. Côte, P. Emery, Phys. Rev. B 74 (2006), 064114.
[27] C. Thomsen, H.T. Grahn, H.J. Maris, J. Tauc, Phys. Rev. B 34 (1986) 4129.
[28] E.D. Palik, Handbook of Optical Constants of Solids, Academic Press, New York, 1991.
[29] A. Nagakubo, 1H. Ogi, H. Ishida, M. Hirao, T. Yokoyama, T. Nishihara, J. Phys. Chem. 118 (2015), 014307.
[30] R.F.S. Hearmon, Solid State Commun. 37 (1981) 915–918.
[31] E.A. Friedman, A.J. Ritger, R.D. Andrews, J. Appl. Phys. 40 (11) (1969) 4243.

A. Devos received a degree in engineering from the Institut Superieur d'Electronique et du Numérique in Lille, France in 1993 and a master's degree in solid state physics from Orsay University the same year. He received his phD in theoretical physics in 1997 from Lille University. Then he joined the group of Dr Bernard Perrin in Paris where he learned a lot about picosecond ultrasonics. He has been senior researcher in French National Center for Scientific Research (CNRS) since 1998 at IEMN in Lille. Current research interests include ultrafast acoustics applied to solid state physics and nanophysics. He is the inventor of the so-called Colored Picosecond Ultrasonic (APiC) technique and he published more than 40 papers and filed 5 patents. He received the CNRS bronze medal in 2008.